ESC European Society of Cardiology

Europace (2025) **27**, euaf021
https://doi.org/10.1093/europace/euaf021

TRANSLATIONAL RESEARCH

Decreased METTL3 in atrial myocytes promotes atrial fibrillation

Jian Shi [1†], Xi-Yu Zhu [1†], Rong-Huang Yu [1], Wen-Xue Liu [1], Jie Yang[1], Lu Tang [1], Chui-Yu Kong [1], Han-Qing Luo [1], Fen Chen [1], Wen-Sen Xie[2], Jia-Lei Fu[2], Jing-Jie Wang [1], Qian Zhou [2*‡], Qing Zhou[1*‡], and Dong-Jin Wang [1*‡]

[1]Department of Cardiothoracic Surgery, Nanjing Drum Tower Hospital, Affiliated Hospital of Medical School, Nanjing University, 321 Zhongshan Road, Nanjing 210000, Jiangsu, China; and [2]Jiangsu Provincial Medical Innovation Center, Affiliated Hospital of Integrated Traditional Chinese and Western Medicine, Nanjing University of Chinese Medicine, Nanjing 210000, China

Received 1 October 2024; accepted after revision 27 January 2025; online publish-ahead-of-print 24 February 2025

Aims Methyltransferase like 3 (METTL3) plays a crucial role in cardiovascular diseases, but its involvement in atrial fibrillation (AF) remains unclear. The study aims to explore the relationship between METTL3 and AF in atrial myocytes.

Methods and results The protein level of METTL3 was evaluated in left atrial appendages (LAAs) from patients with persistent AF and in experimental AF models. cAMP-responsive element modulator (*CREM*) transgenic mice and $CaCl_2$-acetylcholine (ACh)-injected mice were used as AF mice models. Methyltransferase like 3 was globally and atrial conditionally deleted *in vivo* to assess its role in AF. Confocal fluorescence microscopy was employed to examine calcium handling in atrial myocytes. Methylated RNA immunoprecipitation sequencing was performed to identify the downstream target genes of METTL3. Methyltransferase like 3 protein and RNA N6-methyladenosine (m^6A) modification levels were significantly reduced in the LAAs of patients with AF and experimental AF models. Genetic inhibition of METTL3 promoted the development of AF in *CREM* transgenic mice and $CaCl_2$-ACh-injected mice. Knockdown of METTL3 in atrial myocytes resulted in enhanced calcium handling. Reduced METTL3 levels increased SR Ca^{2+}-ATPase Type 2a activity by up-regulating protocadherin gamma subfamily A, 10. Decreased METTL3 protein in atrial myocytes was attributed to down-regulation of cAMP-responsive element-binding protein 1/ubiquitin-specific peptidase 9 X-linked axis.

Conclusion Our study established the pathophysiological role of METTL3 involved in the development of AF and provided a potential mechanism-based target for its treatment.

* Corresponding author. Tel: +86 25 85638721; fax: +86 25 85638721. *E-mail address*: njzhouqian@njucm.edu.cn (Qia.Z.); Tel: +86 25 83106666; fax: +86 25 83106666. *E-mail address:* zhouqing@njglyy.com (Qin.Z.); Tel: +86 25 83106666; fax: +86 25 83106666. *E-mail address:* wangdongjin@njglyy.com (D.-J.W.)
† The first two authors contributed equally to the study.
‡ Qia.Z., Qin.Z., and D.-J.W. shared the corresponding authorship.

Graphical Abstract

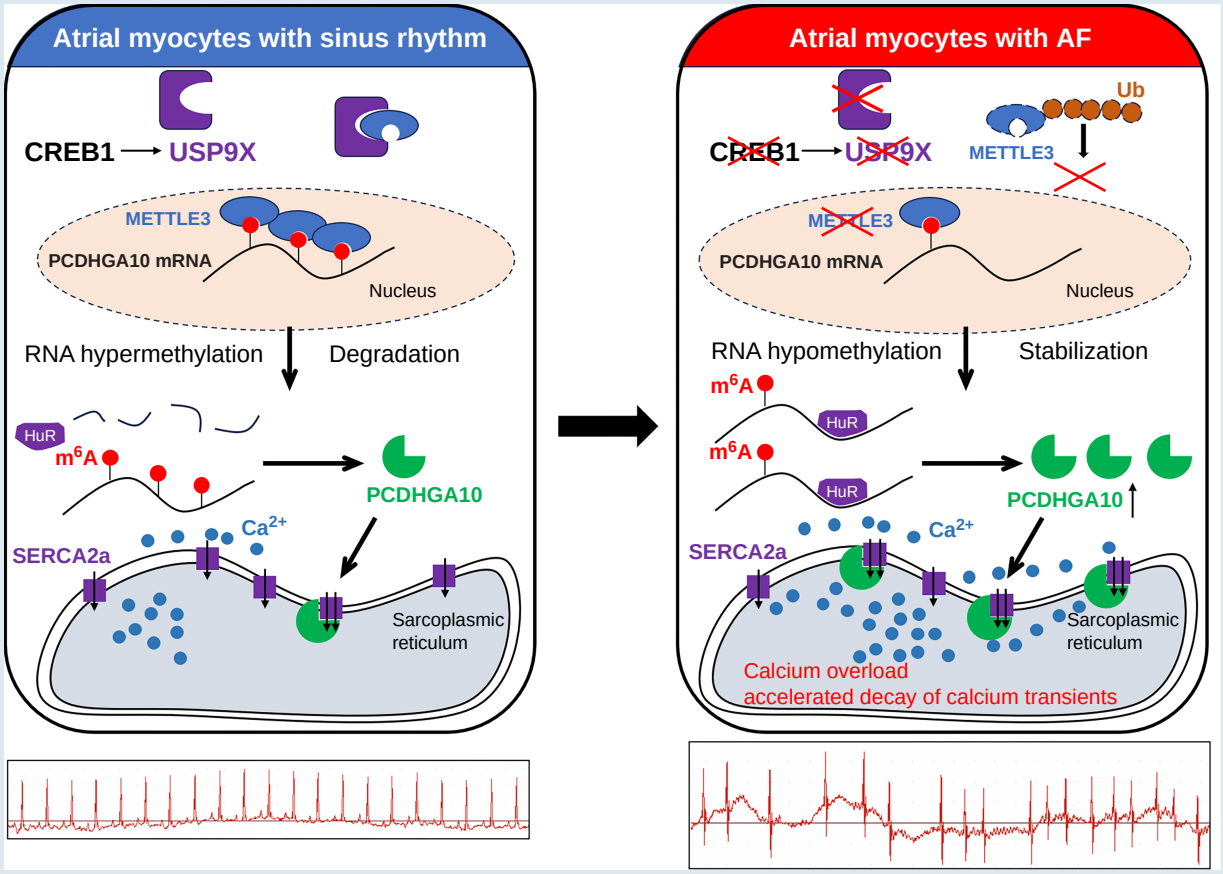

Keywords Atrial fibrillation • m^6A modification • Atrial myocytes • Calcium handling

Translational perspective

Our findings suggested that the CREB1/USP9X/METTL3/protocadherin gamma subfamily A, 10 axis in atrial myocytes plays a crucial role in atrial fibrillation (AF) development by influencing calcium handling. These findings provide insights into potential mechanism-based therapeutic targets for AF treatment.

What's new?

- Atrial fibrillation (AF) is associated with decreased methyltransferase like 3 (METTL3) protein in atrial myocytes.
- Knockdown of METTL3 in atrial myocytes results in abnormal calcium handling and increased susceptibility to AF.
- Protocadherin gamma subfamily A, 10 (PCDHGA10) is regulated by METTL3 and interacts with SR Ca^{2+}-ATPase Type 2a (SERCA2a) in atrial myocytes.

Introduction

Atrial fibrillation (AF) is the most common sustained cardiac arrhythmia,[1] significantly increasing the risk of ischaemia stroke and all-cause mortality.[2,3] The development of AF is typically associated with multiple pathophysiological abnormalities, including atrial structural remodelling, electrical remodelling, and calcium-handling disorder in atrial myocytes.[4] However, the molecular and cellular mechanisms underlying AF remain incompletely understood.[5]

In recent years, research into epigenetic regulatory mechanisms has revealed potential therapeutic targets for AF.[6] N6-methyladenosine (m^6A), the most abundant modification of mRNAs in eukaryotes, plays crucial roles in various cardiovascular diseases.[7] The m^6A modification is catalysed by the methyltransferase complex composed of methyltransferase like 3 (METTL3), methyltransferase like 14 (METTL14), and Wilms' tumour 1–associating protein (WTAP), while it is erased by fat-mass and obesity-associated protein (FTO) or ALKB homologue 5 (ALKBH5), and read by proteins such as YTH N6-methyladenosine RNA-binding protein F2 (YTHDF2), YTHDF3, and Hu-antigen R (HuR).[8] In the fibrotic heart, METTL3 expression has been reported to increase, further promoting cardiac fibroblast proliferation.[9] However, the expression patterns of METTL3 in fibrillating atrial

myocytes and its effects on calcium handling, electrophysiology and AF development are still unclear.

Here, we found that METTL3 and m^{6}A modification levels were down-regulated in the left atrial appendages (LAAs) of patients with AF and experimental AF models. Genetic inhibition of METTL3 promoted AF development in mice by affecting calcium handling of atrial myocytes. Our findings may identify METTL3 as a potential therapeutic target for AF, with important clinical implications.

Methods

Methods are described in full detail in the Supplementary material.

Results

Patient characteristics

The clinical characteristics of patients with sinus rhythm (SR, $n = 19$) and persistent AF ($n = 19$), who were used for dot blot, reverse transcriptase–quantitative polymerase chain reaction (RT–qPCR), western blotting, and immunofluorescence analyses, are summarized in *Table 1*. There were no significant differences between the two groups in terms of age, gender, or comorbidities, such as hypertension and coronary artery disease. However, patients with AF had a larger left atrium. Since these patients underwent a radiofrequency maze procedure, their cardiopulmonary bypass time was significantly longer.

RNA m^{6}A modification and METTL3 protein levels were down-regulated in the left atrial appendages of atrial fibrillation patients and the experimental atrial fibrillation models

To investigate the relationship between m^{6}A modification and AF, we first performed dot blot analysis on patient samples. The result showed that the m^{6}A modification level of total RNA was significantly decreased in the LAAs of patients with AF (*Figure 1A*). HL-1 cells were subjected to tachypacing at indicate frequencies, which caused DNA damage (see Supplementary material online, *Figure S1A*), and were commonly used as the atrial myocytes model of AF.[10,11] Dot

Table 1 The basic clinical information of included patients

	SR ($n = 19$)	AF ($n = 19$)	*P*-value
Age, years (mean ± SD)	54.58 ± 11.29	60.32 ± 8.83	0.09[a]
Male (*n*, %)	13, 68.4%	11, 57.9%	0.501[b]
BMI (mean ± SD)	24.24 ± 3.96	23.96 ± 2.90	0.812[a]
Hypertension (*n*, %)	6, 31.0%	5, 26.3%	0.721[b]
Diabetes (*n*, %)	1, 5.3%	1, 5.3%	1[b]
CAD (*n*, %)	4, 21.1%	2, 10.5%	0.374[b]
Smoke (*n*, %)	3, 15.8%	2, 10.5%	0.631[b]
Drink (*n*, %)	1, 5.3%	2, 10.5%	0.547[b]
LAD, cm (mean ± SD)	4.18 ± 0.60	4.86 ± 0.69	*0.006*[a]
EF, % (mean ± SD)	56.09 ± 8.66	55.56 ± 4.19	0.817[a]
Blood transfusion, mL [median (IQRs)]	25 (0–612.5)	0 (0–300)	0.205[c]
Operation time, min [median (IQRs)]	220 (168.75–242.50)	250 (210.00–295.00)	0.086[b]
CPB time, min [median (IQRs)]	108.5 (77.25–144.25)	132 (127.00–158.00)	*0.045*[c]
NYHA Ⅰ (*n*, %)	2, 10.5%	2, 10.5%	0.455[b]
Ⅱ (*n*, %)	9, 47.4%	5, 26.3%	
Ⅲ (*n*, %)	8, 42.1%	11, 57.9%	
Ⅳ (*n*, %)	0, 0%	1, 5.3%	
CRP, mg/L [median (IQRs)]	3.1 (2.175– 4.125)	2.9 (2.450–4.600)	0.13[c]
Hb, g/L [median (IQRs)]	129.5 (114.25–145.00)	147.0 (133.00–154.00)	0.307[c]
ALT, U/L [median (IQRs)]	18.8 (14.050–30.575)	19.1 (14.375–51.625)	0.353[c]
TBA, μmol/L [median (IQRs)]	2.95 (2.550–5.275)	4.45 (2.025–7.500)	0.702[c]
Scr, μmol/L [median (IQRs)]	66 (55.50–77.75)	57 (55.25–69.50)	0.87[c]
BUN, mmol/L [median (IQRs)]	6.4 (5.425–6.925)	5.75 (5.425–6.400)	0.382[c]
BNP, pg/mL [median (IQRs)]	115.5 (30.35–247.00)	175.0 (66.00–270.25)	0.237[c]

Italics indicate that the $P < 0.05$, indicating a significant difference.
ALT, alanine transaminase; BMI, body mass index; BUN, blood urea nitrogen; CAD, coronary heart disease; CPB, cardiopulmonary bypass; CRP, C-reactive protein; EF, ejection fraction; Hb, haemoglobin; IQRs, 25th–75th percentile; LAD, left atrial diameter; Scr, serum creatinine; TBA, total bile acid.
[a]Comparisons were made using unpaired Student's *t*-test
[b]Comparisons were made using the χ^2 test or the Fisher's test.
[c]Comparisons were made using non-parametric Mann–Whitney test.

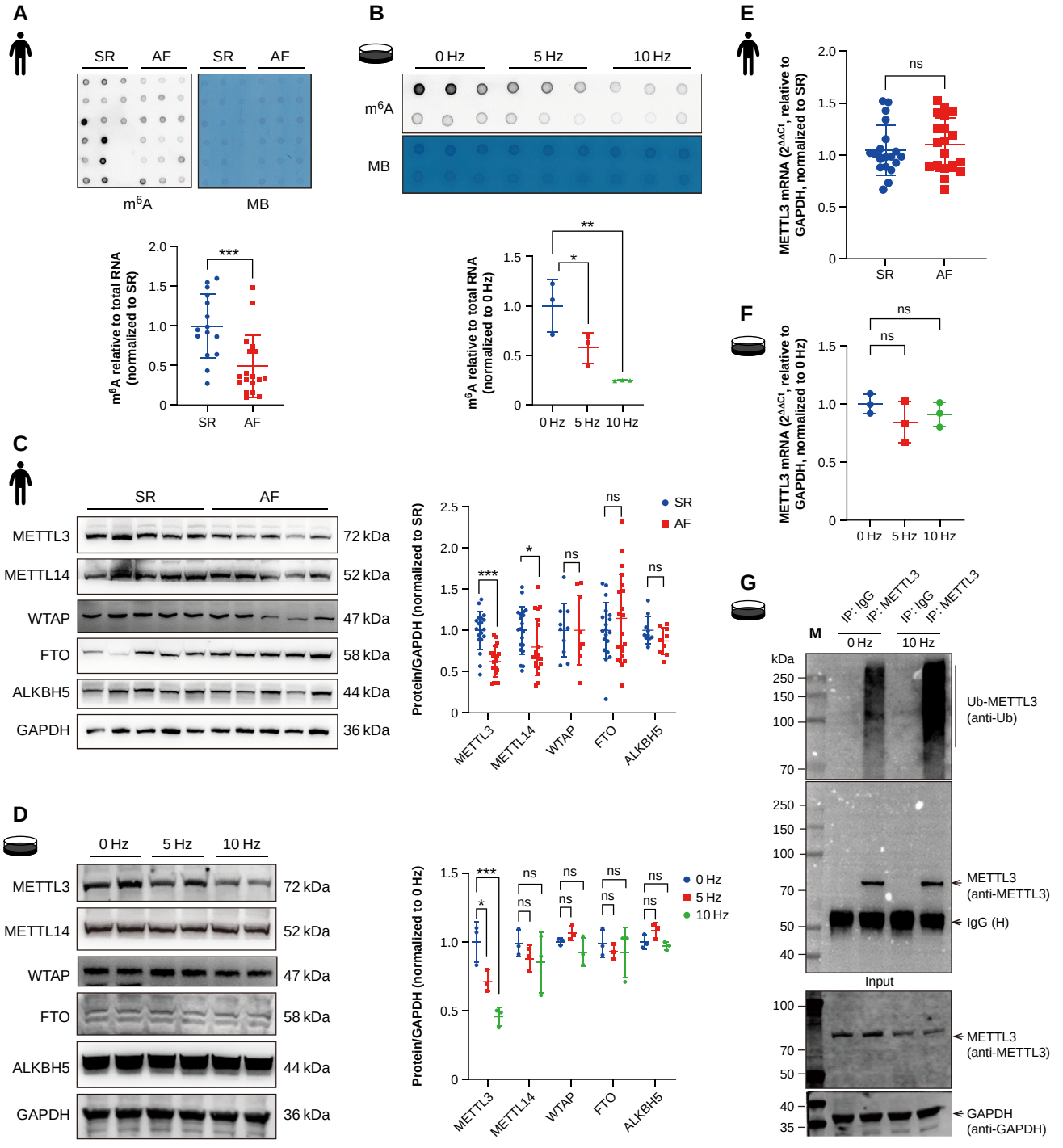

Figure 1 M6a modification and METTL3 were down-regulated in AF. (*A*) Dot blot analysis was used to assess the m^{6}A modification levels in total RNA (500 ng) from LAA tissues of patients with SR ($n = 15$) and AF ($n = 18$). Data are presented as mean ± SD. ***$P < 0.001$, comparison made using an unpaired Student's *t*-test. m^{6}A, anti-m^{6}A antibody; MB, methylene blue staining. (*B*) Dot blot analysis of m^{6}A modification levels in total RNA from HL-1 cells at varying stimulation frequencies, with loading amounts of 250 ng (up) and 125 ng (down). The graph below shows the statistical analysis results at RNA loading amount of 250 ng. Data are presented as mean ± SD. 0 Hz ($n = 3$), 5 Hz ($n = 3$), and 10 Hz ($n = 3$). *$P < 0.05$, **$P < 0.01$, comparisons made using ordinary one-way ANOVA. (*C*) Protein expression of methyltransferases METTL3, METTL14, WTAP, and demethylase FTO, ALKBH5 in LAA tissue of patients with AF. Data are presented as mean ± SD. Sinus rhythm ($n = 10$–19), AF ($n = 9$–19). *$P < 0.05$, ***$P < 0.001$, comparisons made using unpaired Student's *t*-test. (*D*) Protein expression of methyltransferases METTL3, METTL14, WTAP, and demethylase FTO, ALKBH5 in HL-1 cells at different stimulation frequencies. Data are presented as mean ± SD. 0 Hz ($n = 3$), 5 Hz ($n = 3$), and 10 Hz ($n = 3$). *$P <$ 0.05, ***$P < 0.001$, comparisons made using ordinary one-way ANOVA. (*E*) METTL3 mRNA levels were detected by RT–qPCR in patients with AF. Data are presented as mean ± SD. Sinus rhythm ($n = 19$), AF ($n = 19$), comparison made using unpaired Student's *t*-test; (*F*) METTL3 mRNA levels

(continued)

blot and immunofluorescence results showed that the m^{6}A modification of HL-1 cells progressively decreased with increasing stimulation frequency (*Figure 1B* and see Supplementary material online, *Figure S1B*).

Given that m^{6}A modification is catalysed by METTL3–METTL14–WTAP complex and demethylated by FTO or ALKBH5, we assessed the protein levels of these enzymes in the LAAs of patients with AF and in cell models via western blotting. The results revealed that only the protein levels of METTL3 and METTL14 were significantly downregulated in the LAAs of patients with AF (*Figure 1C*). In AF cell models, only the METTL3 protein level was reduced (*Figure 1D*). These findings were confirmed by immunofluorescence analyses (see Supplementary material online, *Figure S1C* and *D*). In the left atria of mice with $CaCl_2$-acetylcholine (ACh)-induced AF, METTL3 expression was also significantly decreased (see Supplementary material online, *Figure S1E*).

Subsequently, we focused on the role of METTL3 in atrial myocytes in the context of AF. Reverse transcriptase–qPCR analysis showed no significant change in METTL3 mRNA levels in AF patient samples or cell models (*Figure 1E* and *F*), leading us to hypothesize that METTL3 protein degradation is accelerated during AF progression. To determine whether METTL3 degradation in atrial cardiomyocytes primarily relies on the proteasomal or lysosomal pathway, we treated HL-1 cells with the proteasome inhibitor MG132 or the lysosomal inhibitor chloroquine. The results demonstrated that METTL3 accumulated in cells treated with MG132 but not in those treated with chloroquine (see Supplementary material online, *Figure S1F*), suggesting that METTL3 in atrial myocytes was predominantly degraded via the proteasomal pathway. Additionally, Co-immunoprecipitation/western blotting experiments showed that the ubiquitination level of METTL3 was significantly increased in AF cell models (*Figure 1G*). These findings suggest that the reduction of METTL3 and its mediated m^{6}A modification in atrial myocytes is closely linked to the onset of AF.

METTL3 deletion promoted $CaCl_2$-acetylcholine-induced atrial fibrillation and spontaneous atrial fibrillation in *CREM* mice

To investigate the impact of METTL3 on AF, we induced AF by injecting $CaCl_2$-ACh into the tail vein of wild-type (WT) and *Mettl3*$^{+/-}$ mice for 2 weeks (see Supplementary material online, *Figure S2A*).[12–14] Genotype identification of WT and *Mettl3*$^{+/-}$ mice was confirmed via PCR analysis (see Supplementary material online, *Figure S2B*). Compared with WT mice, both the mRNA and protein levels of METTL3 in the atria of *Mettl3*$^{+/-}$ mice were significantly reduced (*Figure 2A* and *B*). Electrocardiogram (ECG) results showed that heterozygous deletion of METTL3 significantly increased the duration of $CaCl_2$-ACh-induced AF (*Figure 2C*).

With cardiomyocyte-specific expression of CREM-IbΔC-X (an isoform of CREM in human), *CREM* mice are a widely used transgenic mouse model of AF.[15–17] These mice progressively develop atrial dilation, atrial fibrosis, and spontaneous AF with age (see Supplementary material online, *Figure S3*). To test whether loss of METTL3 in atrial myocytes promotes the development of spontaneous AF, we generated *Mettl3*$^{flox/flox}$*:CREM* double-mutant (DM) mice and injected them with AAV9-Anf-Zsgreen or AAV9-Anf-Cre virus[18] (*Figure 2D*). Genotyping of DM mice was confirmed via PCR analysis (see Supplementary material online, *Figure S4A and B*). Atrial-specific expression of the virus was validated by the presence of fluorescence signals in the atrium but not the ventricle of *Tg-tdTomato* mice 4 weeks after AAV9-Anf-Cre virus injection (see Supplementary material online, *Figure S4C*). Four weeks post-injection in DM mice, METTL3 protein levels were significantly reduced in the atrium but not in the ventricle and liver (*Figure 2E*). Electrocardiogram monitoring revealed that atrial-specific deletion of METTL3 in *CREM* mice increased the occurrence of spontaneous AF within 8 weeks (*Figure 2F*). These findings suggested that both global and atrial myocyte-specific deletion of METTL3 promotes AF development.

Neither atrial myocyte-specific deletion nor global heterozygous deletion of METTL3 caused atrial structural remodelling such as atrial enlargement or fibrosis (see Supplementary material online, *Figure S5*). Since ACh activates the ACh-sensitive potassium channels ($I_{K,ACh}$) of atrial myocytes, shortening action potential duration and promoting AF,[19,20] we examined the mRNA expression of KCNJ3 and KCNJ5 (potassium inwardly rectifying channel Subfamily J Members 3 and 5, the subunits of potassium channels) in the atrial tissues of *Mettl3*$^{+/-}$ mice via RT–qPCR. The results showed that KCNJ5 mRNA was significantly increased, while KCNJ3 mRNA was unchanged (*Figure 3A*). Western blotting confirmed that KCNJ5 protein was significantly elevated in the right atrial appendage (*Figure 3B*), a finding consistent with results from AF patient samples (*Figure 3C*). Additionally, KCNJ5 expression was also significantly upregulated in AF cell models (*Figure 3D* and *E*), consistent with the results of METTL3 knockdown (see Supplementary material online, *Figure S6A*). *In vitro* electrophysiological experiments showed that knockdown of METTL3 increased ACh-sensitive potassium current ($I_{K,ACh}$) (see Supplementary material online, *Figure S6B* and *C*).

Knockdown of METTL3 resulted in abnormal calcium handling in atrial myocytes

In addition to changes in ion channels expression, calcium handling in atrial myocytes is also involved in the pathogenesis of AF.[1] To investigate whether METTL3 affects calcium handling, we knocked down METTL3 in primary neonatal mice atrial myocytes (NMAMs) (*Figure 4A* and *B*). This resulted in a reduction of m^{6}A modification levels in the NMAMs (*Figure 4C*). Calcium transient measurement in these atrial myocytes, paced at 1 Hz, showed that METTL3 knockdown increased amplitude and shortened the decay time of the calcium transients (*Figure 4D*).

Next, we isolated primary adult mice atrial myocytes (AMAMs) from WT and *Mettl3*$^{+/-}$ mice using Langendorff perfusion and performed calcium transient analysis. In AMAMs, the decay of calcium transients was also significantly accelerated (*Figure 4E*). However, key calcium-handling proteins, including NCX1, SR Ca^{2+}-ATPase

Figure 1 Continued

in HL-1 cells at certain stimulation frequencies. Data are presented as mean ± SD. 0 Hz ($n = 3$), 5 Hz ($n = 3$), and 10 Hz ($n = 3$), comparison made using ordinary one-way ANOVA; (*G*) Endogenous immunoprecipitation (IP) performed on 0 or 10 Hz paced HL-1 cells using METTL3 antibody or negative control rabbit IgG. Western blotting was then performed using the corresponding antibodies; Co-IP/western blotting experiments revealed that 10 Hz stimulation significantly increased the ubiquitination level of METTL3. AF, atrial fibrillation; ANOVA, analysis of variance; LAA, left atrial appendages; METTL3, methyltransferase like 3; GAPDH, glyceraldehyde-3-phosphate dehydrogenase; ns, not significant; RT–qPCR, reverse transcriptase–quantitative polymerase chain reaction; SD, standard deviation; SR, sinus rhythm.

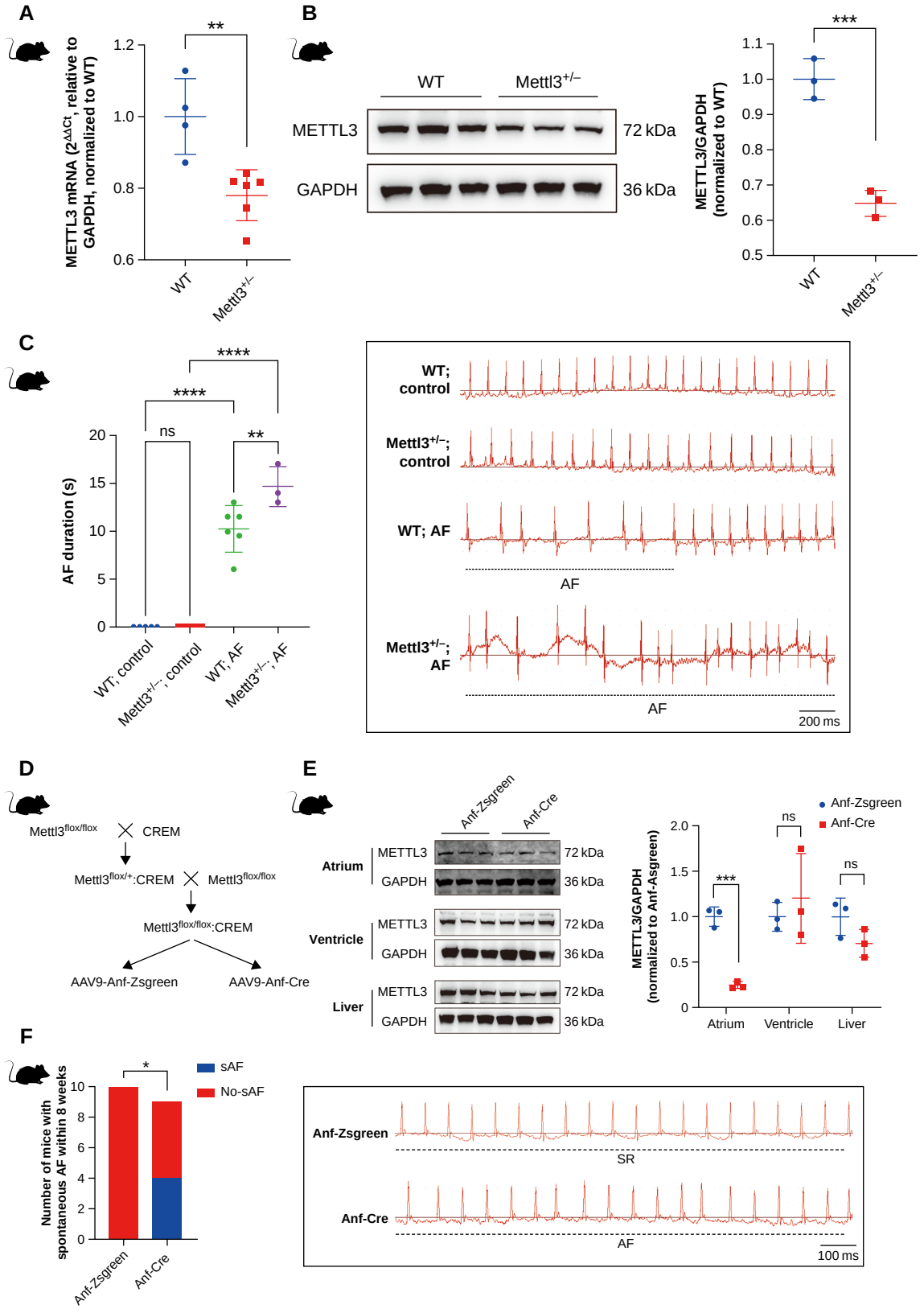

Figure 2 METTL3 deletion promoted $CaCl_2$-ACh-induced AF and spontaneous AF in *CREM* mice. (*A*) RT–qPCR was used to detect the expression of METTL3 mRNA in the atrium of *Mettl3*$^{+/-}$ mice. Data are presented as mean ± SD. WT ($n = 4$), *Mettl3*$^{+/-}$ ($n = 6$). $^{**}P < 0.01$, comparison made using unpaired Student's *t*-test. (*B*) Western blotting was used to detect expression of METTL3 protein in the atrium of *Mettl3*$^{+/-}$ mice. Data

(continued)

Type 2a (SERCA2a), phospholamban (PLN), and the phosphorylation of PLN at pS16 and pT17, did not exhibit significant changes in METTL3 knockdown HL-1 cells or the atrial tissues of *Mettl3*$^{+/-}$ mice (see Supplementary material online, *Figure S7*).

METTL3 affects calcium handling in atrial myocytes through protocadherin gamma subfamily A, 10 via an m^{6}A-HuR-mediated pathway

METTL3 catalyses the m^{6}A modification of target mRNA, affecting their splicing, maturation, nuclear export, translation, and stability, thereby influencing target genes expression.[21] To identify the target genes regulated by METTL3 during AF, we performed methylated RNA immunoprecipitation sequencing (MeRIP-Seq) in the atrial myocyte model of AF. We focused on genes that showed reduced m^{6}A modification and altered transcription levels. Cross-analysis of m^{6}A modification and transcription levels revealed that m^{6}A modification levels of Gm6842, 9330104G04Rik, and protocadherin gamma subfamily A, 10 (PCDHGA10) were significantly decreased, while their transcription levels were significantly increased (*Figure 5A* and Supplementary material online, Appendix *S2*). Since Gm6842 is a pseudogene and 9330104G04Rik is a non-coding RNA with no human homologue, we focused on PCDHGA10 for further investigation.

We first knocked down METTL3 in the HL-1 cells and performed MeRIP-qPCR. The results showed a significant reduction in the m^{6}A modification level of PCDHGA10 and a significant increase in its transcription levels, consistent with findings in the AF cell model (*Figure 5B* and *C*). Overexpression of METTL3 led to a decrease in PCDHGA10 transcript levels (*Figure 5C*), and a corresponding reduction in PCDHGA10 protein levels (*Figure 5D*). Furthermore, PCDHGA10 protein level was significantly elevated in LAAs of patients with AF (*Figure 5E*). The m^{6}A peak map combined with the SRAMP database identified multiple m^{6}A modification sites in the PCDHGA10 mRNA in both mouse and human (see Supplementary material online, *Figure S8A* and *B*). Combining the BLAST results on the NCBI database, eight conserved m^{6}A modification sites on the mouse and human PCDHGA10 genes were found (see *Supplementary Appendix 3* and see Supplementary material online, *Figure S8C*).

While YTHDF2 and YTHDF3 are well-established m^{6}A readers that promote mRNA degradation,[22] their knockdown in HL-1 cells did not result in an increase in PCDHGA10 (*Figure 5F*). Additionally, HuR was found to bind to and stabilize mRNA with less m^{6}A modification and knocking it down caused PCDHGA10 to decrease (*Figure 5G*). RNA immunoprecipitation combined with PCR (RIP-PCR) revealed increased binding of HuR to PCDHGA10 mRNA following METTL3 knockdown (*Figure 5H*). Together, these results suggested that METTL3 repressed PCDHGA10 in an m^{6}A-HuR-mediated pathway.

Next, to determine whether PCDHGA10 regulates calcium handling in atrial myocytes, we overexpressed PCDHGA10 in NMAMs. Calcium-handling assays showed that PCDHGA10 overexpression significantly enhanced amplitude and accelerated decay of calcium transients (*Figure 6A*), replicating the effects seen with METTL3 knockdown. Furthermore, knockdown of PCDHGA10 in NMAMs alleviated the abnormal calcium handling caused by METTL3 knockdown (*Figure 6B*).

Protocadherin gamma subfamily A, 10 is a member of the protocadherin γ gene cluster (Pcdhg-γ), which encodes cadherin-like transmembrane proteins[23,24] and may not directly act as a calcium ion channel. Literature suggests that Pcdhg-γ proteins interact with calcium-handling proteins, such as SERCA2a.[25] We used lentivirus to overexpress PCDHGA10-GFP in HL-1 cells and performed immunofluorescence experiments. The result confirmed that PCDHGA10 co-localized with SERCA2a and the sarcoplasmic reticulum (*Figure 6C*). Co-immunoprecipitation/western blotting experiments in HEK293T cells transfected with PCDHGA10-GFP and Flag-SERCA2a plasmids further confirmed the interaction between PCDHGA10 and SERCA2a (*Figure 6D*). To explore whether PCDHGA10 affects the SERCA2a activity, we measured SERCA2a-ATPase activity and found that it was significantly increased in PCDHGA10-overexpressing HL-1 cells (*Figure 6E*). Moreover, knockdown of PCDHGA10 prevented the increase in SERCA2a-ATPase activity induced by METTL3 knockdown (*Figure 6F*). During diastole of atrial myocytes, Ca^{2+} is taken back up into the sarcoplasmic reticulum via SERCA2a, or extruded from cell via NCX1.[26,27] To explore whether NCX1 activity was altered, caffeine was applied, which maintains the ryanodine receptor 2 (RyR2) open.[28,29] All calcium pumped back into the SR will be immediately released by the open RyR2 channels, making SERCA pumping inefficient. Therefore, the decay rate of caffeine-induced calcium transients depends only on extrusion by NCX1, which remained unchanged in METTL3 or PCDHGA10 knockdown NMAMs. Additionally, PCDHGA10 knockdown restored the increased amplitude (reflecting sarcoplasmic reticulum calcium load) caused by METTL3 deficiency (see Supplementary material online, *Figure S9*). The above results indicated that decreased METTL3 led to increased PCDHGA10 expression, which in turn enhanced SERCA2a activity and increased sarcoplasmic reticulum calcium load in atrial myocytes.

Figure 2 Continued

are presented as mean ± SD. WT ($n = 3$); *Mettl3*$^{+/-}$ ($n = 3$). ***$P < 0.001$, comparison made using unpaired Student's *t*-test. (*C*) Duration of induced AF in each group of mice following $CaCl_2$-ACh injection (left). The representative ECG of the limb leads from each group of mice (right). WT; control ($n = 5$): WT mice injected with saline, *Mettl3*$^{+/-}$; control ($n = 5$): *Mettl3*$^{+/-}$ mice injected with saline, WT; AF ($n = 6$): WT mice injected with $CaCl_2$-ACh, *Mettl3*$^{+/-}$; AF ($n = 3$): *Mettl3*$^{+/-}$ mice injected with $CaCl_2$-ACh. Data are presented as mean ± SD. **$P < 0.01$, ****$P < 0.0001$, comparison made using two-way ANOVA. (*D*) Schematic diagram illustrating the process of specific METTL3 knockout in atrial myocytes of *CREM* mice. Parental *Mettl3*$^{flox/flox}$ mice were crossed with *CREM* mice to generate *Mettl3*$^{flox/+}$:*CREM* mice, which were then bred with *Mettl3*$^{flox/flox}$ mice to obtain *Mettl3*$^{flox/flox}$:*CREM* mice. These mice were then injected with AAV9-Anf-Cre virus to specifically knock out METTL3 in atrial myocytes. The *Mettl3*$^{flox/flox}$:*CREM* mice injected with AAV9-Anf-Zsgreen virus served as controls. (*E*) Expression of METTL3 protein in the atrium, ventricle, and liver of *Mettl3*$^{flox/flox}$:*CREM* mice was evaluated by western blotting assay 4 weeks after AAV9-Anf virus injection. Data are represent as mean ± SD. AAV9-Anf-Zsgreen ($n = 3$), AAV9-Anf-Cre ($n = 3$). ***$P < 0.001$, comparisons made using unpaired Student's *t*-test. (*F*) Statistics of spontaneous AF in *Mettl3*$^{flox/flox}$:*CREM* mice 4 weeks after AAV9-Anf virus injection (left). Schematic diagram of limb lead ECG (right). Data represent the number of mice with or without sAF. AAV9-Anf-Zsgreen ($n = 10$), AAV9-Anf-Cre ($n = 9$). *$P < 0.05$, comparison made using the Fisher's test. AF, atrial fibrillation; ANOVA, analysis of variance; CREM, cAMP-responsive element modulator; ECG, electrocardiogram; METTL3, methyltransferase like 3; GAPDH, glyceraldehyde-3-phosphate dehydrogenase; ns, not significant; sAF, spontaneous atrial fibrillation; SD, standard deviation; WT, wild-type.

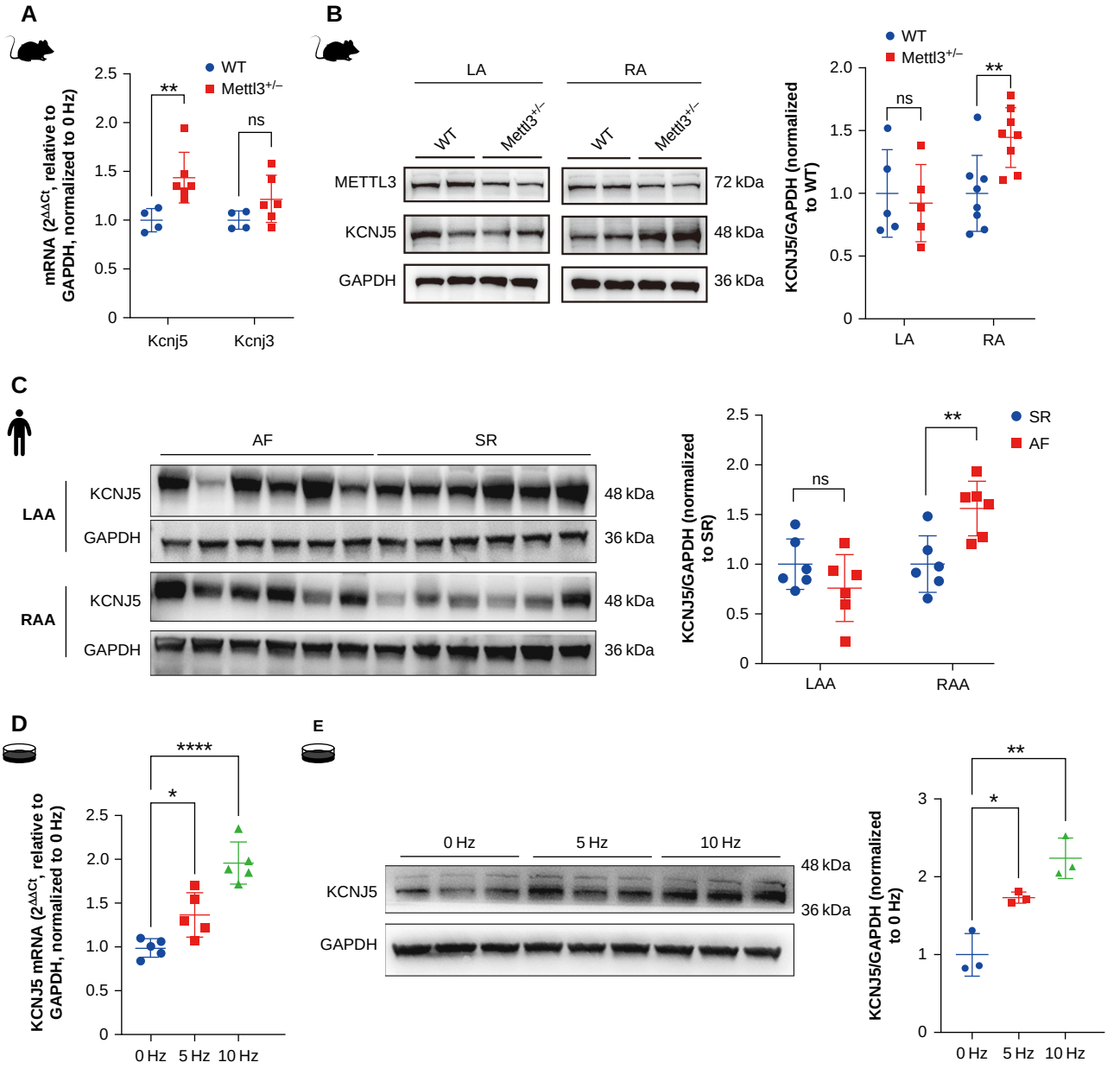

Figure 3 METTL3 deficiency increased KCNJ5 expression in the right atrium. (*A*) RT–qPCR was used to evaluate expression of KCNJ3 and KCNJ5 mRNA in bilateral atria of *Mettl3*$^{+/-}$ mice. Data are represented as mean ± SD. WT ($n = 4$), *Mettl3*$^{+/-}$ ($n = 6$). $^{**}P < 0.01$, comparisons made using unpaired Student's *t*-test. (*B*) Western blotting was used to evaluate KCNJ5 protein expression in bilateral atria of *Mettl3*$^{+/-}$ mice. Data are represented as mean ± SD. WT left atrium (LA) ($n = 5$), *Mettl3*$^{+/-}$ LA ($n = 5$), WT right atrium (RA) ($n = 8$), *Mettl3*$^{+/-}$ RA ($n = 8$). $^{**}P < 0.01$, comparisons made using unpaired Student's *t*-test. (*C*) KCNJ5 protein expression levels were detected by western blotting in bilateral atrial appendages from patients with AF and SR. Data are represented as mean ± SD. SR ($n = 6$), AF ($n = 6$). $^{**}P < 0.01$, comparisons made using unpaired Student's *t*-test; (*D*) KCNJ5 mRNA expression levels were detected by RT–qPCR at certain stimulation frequencies in AF cell models. Data are represented as mean ± SD. 0 Hz ($n = 5$), 5 Hz ($n = 5$), and 10 Hz ($n = 5$). $^{*}P < 0.05$, $^{****}P < 0.0001$, comparison made using ordinary one-way ANOVA. (*E*) KCNJ5 protein expression levels were detected at certain stimulation frequencies in AF cell models. Data are represented as mean ± SD. 0 Hz ($n = 3$), 5 Hz ($n = 3$), and 10 Hz ($n = 3$). $^{*}P < 0.05$, $^{**}P < 0.01$, comparisons made using ordinary one-way ANOVA. AF, atrial fibrillation; ANOVA, analysis of variance; LAA, left atrial appendages; METTL3, methyltransferase like 3; GAPDH, glyceraldehyde-3-phosphate dehydrogenase; ns, not significant; RAA, right atrial appendage; RT–qPCR, reverse transcriptase–quantitative polymerase chain reaction; SD, standard deviation; SR, sinus rhythm; WT, wild type.

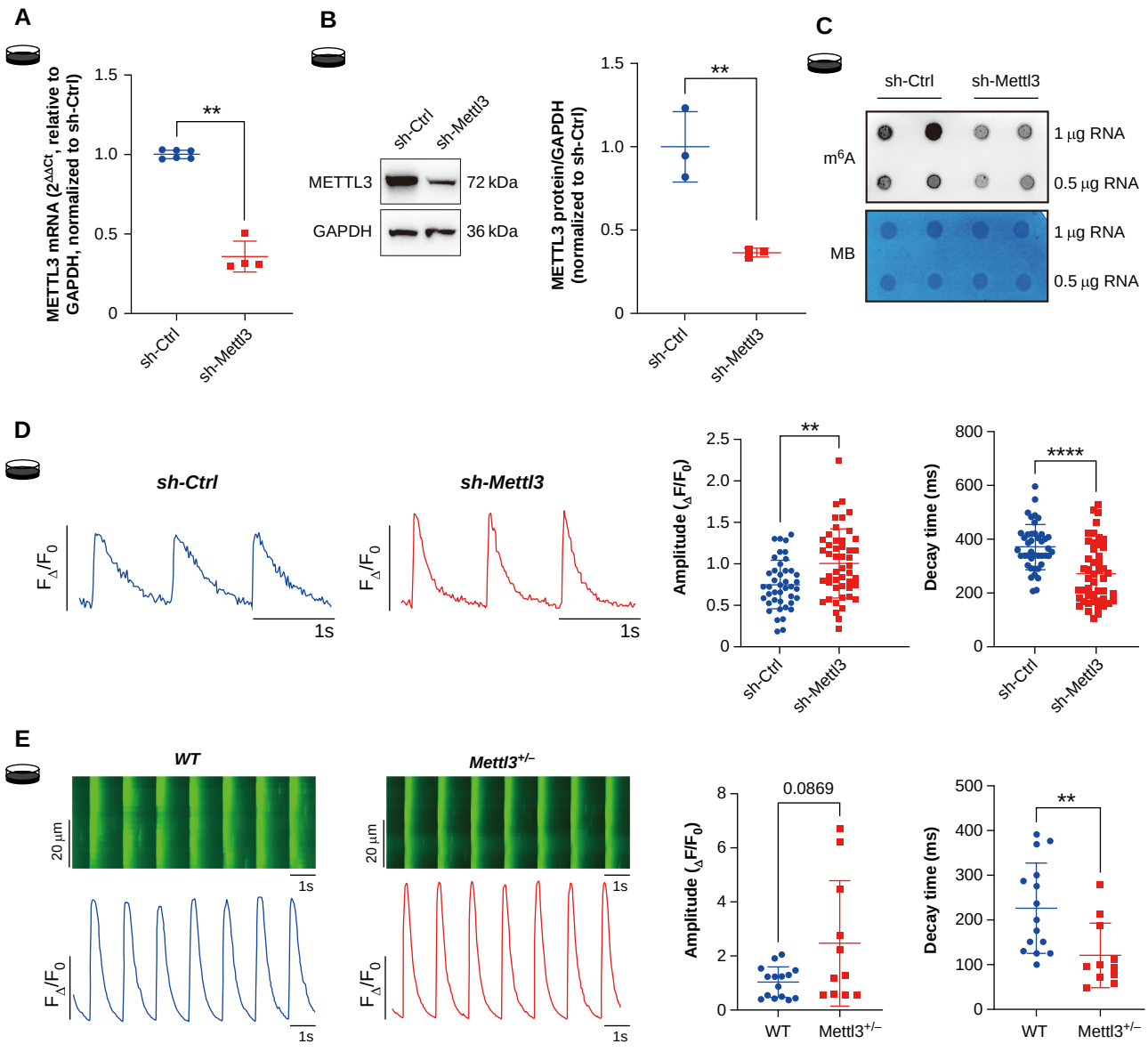

Figure 4 METTL3 deficiency resulted in accelerated decay of calcium transients in atrial myocytes. (*A*) Expression of METTL3 mRNA was determined by RT–qPCR in NMAMs infected with knockdown lentivirus. Data are represent as mean ± SD. Sh-Ctrl ($n = 6$), sh-Mettl3 ($n = 4$). $^{**}P < 0.01$, comparisons made using unpaired Student's *t*-test. (*B*) Expression of METTL3 protein was determined by western blotting in NMAMs infected with knockdown lentivirus. Data are represented as mean ± SD. Sh-Ctrl ($n = 3$), sh-Mettl3 ($n = 3$). $^{**}P < 0.01$, comparisons made using unpaired Student's *t*-test. (*C*) N6-methyladenosine modification levels were detected by dot blot assay in METTL3 knockdown NMAMs. (*D*) Calcium transients were measured in METTL3 knockdown NMAMs using confocal microscopy. Data are represent as mean ± SD. Sh-Ctrl ($n = 42$ cells from three technical replicates), sh-Mettl3 ($n = 48$ cells from three technical replicates). $^{**}P < 0.01$, $^{****}P < 0.0001$, comparisons made using unpaired Student's *t*-test. (*E*) Calcium transients in AMAMs were detected by the confocal microscopy. Data are represented as mean ± SD. WT ($n = 15$ cells from three mice), *Mettl3*$^{+/-}$ ($n = 11$ cells from three mice). $^{**}P < 0.01$, comparisons made using non-parametric Mann–Whitney test (for amplitude) and unpaired Student's *t*-test (for decay time). AMAMs, adult mice atrial myocytes; m^{6}A, N6-methyladenosine; MB, methylene blue staining; METTL3, methyltransferase like 3; GAPDH, glyceraldehyde-3-phosphate dehydrogenase; NMAMs, neonatal mice atrial myocytes; RT–qPCR, reverse transcriptase–quantitative polymerase chain reaction; SD, standard deviation; WT, wild type.

CREB1/USP9X regulates protein level of METTL3

We next explored the mechanisms underlying the down-regulation of METTL3 protein during AF. Studies have suggested that reduced expression and transcriptional activity of CREB1 are associated with AF.[30,31] *CREM* mice, which overexpress the transcriptional repressor CREM-IbΔC-X, also show impaired CREB1 function.[15,32] To investigate this, we examined CREB1 and its phosphorylated form (p-CREB1) in LAA samples from patients with AF. Both CREB1 protein expression and p-CREB1 (S133) were significantly reduced in AF (*Figure* 7*A*). We also found that CREB1 expression was decreased in AF cell models (*Figure* 7*B*). Knockdown of CREB1 in HL-1 cells resulted in a significant

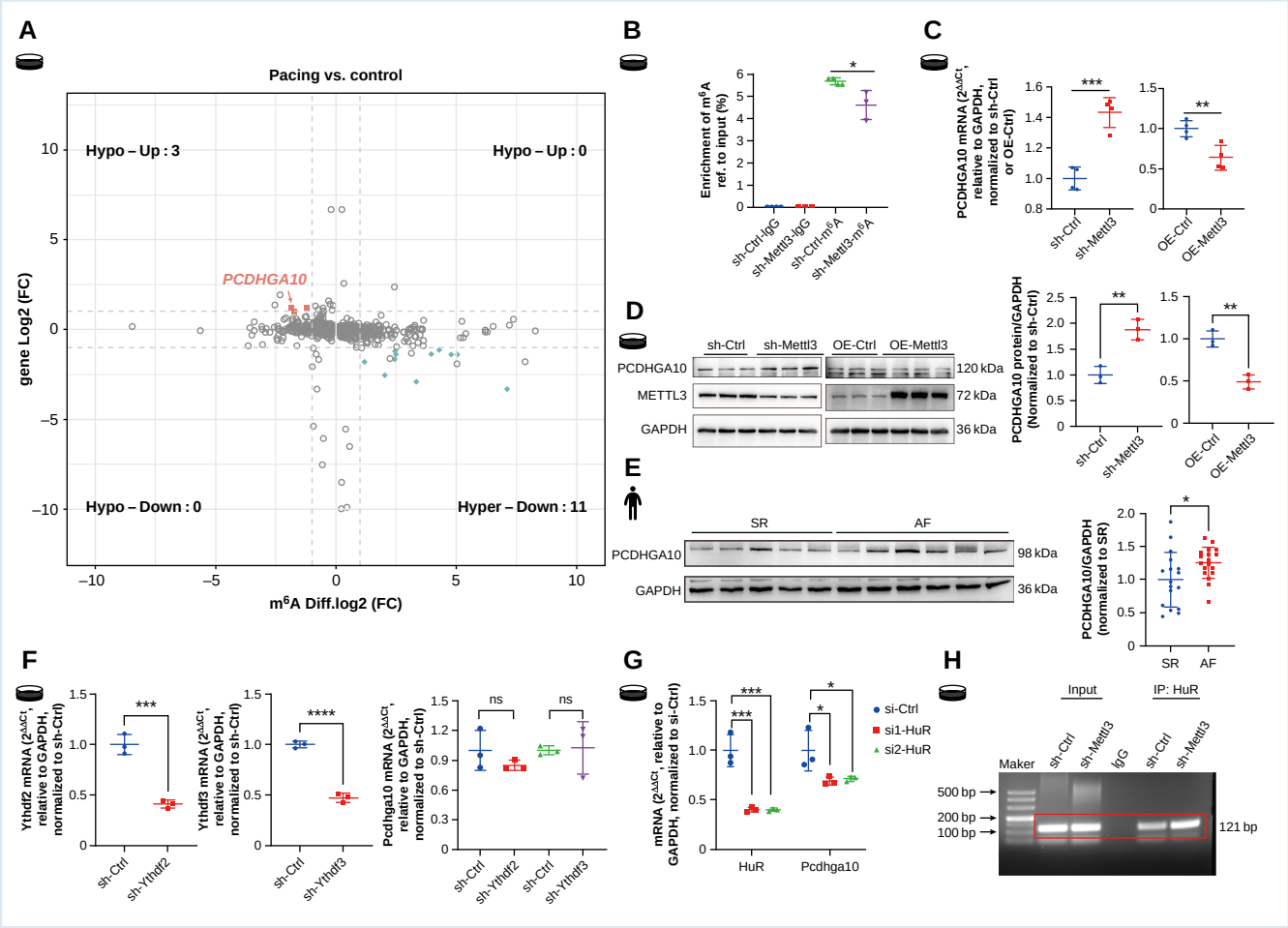

Figure 5 PCDHGA10 was regulated by METTL3. (*A*) MeRIP-Seq in the AF cell model showed reduced m^{6}A modification and increased transcript levels of PCDHGA10. Ten Hertz paced HL-1 cells served as the experimental group ($n = 3$), and HL-1 cells without pacing served as the control group ($n = 3$). (*B*) MeRIP-qPCR was used to validate that m^{6}A modifications on PCDHGA10 mRNA were regulated by METTL3. Fragments of RNA from sh-Ctrl or sh-Mettl3 HL-1 cells were enriched with m^{6}A or rabbit IgG antibody, followed by reverse transcription and qPCR assay. Data are represented as mean ± SD. Sh-Ctrl ($n = 4$), sh-Mettl3 ($n = 3$). *$P < 0.05$, comparison made using two-way ANOVA. (*C*) PCDHGA10 mRNA expression was evaluated by RT–qPCR in sh-Mettl3 or OE-Mettl3 HL-1 cells. Data are represented as mean ± SD. Sh-Ctrl ($n = 4$), sh-Mettl3 ($n = 4$), OE-Ctrl ($n = 4$), and OE-Mettl3 ($n = 4$). **$P < 0.01$, ***$P < 0.001$, comparisons made using unpaired Student's *t*-test. (*D*) Protocadherin gamma subfamily A, 10 protein expression was evaluated by western blotting in sh-Mettl3 or OE-Mettl3 HL-1 cells. Data are represented as mean ± SD. Sh-Ctrl ($n = 3$), sh-Mettl3 ($n = 3$), OE-Ctrl ($n = 3$), and OE-Mettl3 ($n = 3$). **$P < 0.01$, comparisons made using unpaired Student's *t*-test. (*E*) Protein expression of PCDHGA10 was evaluated by western blotting in LAA tissue of patients with AF. Data are represented as mean ± SD. SR ($n = 17$), AF ($n = 18$). *$P < 0.05$, comparison made using non-parametric Mann–Whitney test. (*F*) Ythdf2, Ythdf3, and Pcdhga10 mRNA were evaluated by RT–qPCR in sh-Ythdf2 or sh-Ythdf3 HL-1 cells. Data are represented as mean ± SD. Sh-Ctrl ($n = 3$), sh-Ythdf2 ($n = 3$), and sh-Ythdf3 ($n = 3$). ***$P < 0.001$, ****$P < 0.0001$, comparisons made using unpaired Student's *t*-test. (*G*) HuR and Pcdhga10 mRNA were evaluated by RT–qPCR in si-HuR HL-1 cells. si-Ctrl ($n = 3$), si1-HuR ($n = 3$), and si2-HuR ($n = 3$). *$P < 0.05$, ***$P < 0.001$, comparisons made using ordinary one-way ANOVA. (*H*) RIP-PCR was used to detect the enrichment of PCDHGA10 mRNA by HuR protein under the condition of METTL3 knockdown in HL-1 cells. AF, atrial fibrillation; ANOVA, analysis of variance; FC, fold change; GAPDH, glyceraldehyde-3-phosphate dehydrogenase; LAA, left atrial appendage; m^{6}A, N6-methyladenosine; MeRIP-Seq, methylated RNA immunoprecipitation sequencing; METTL3, methyltransferase like 3; ns, not significant; PCDHGA10, protocadherin gamma subfamily A, 10; RT–qPCR, reverse transcriptase–quantitative polymerase chain reaction; SD, standard deviation; SR, sinus rhythm; Ythdf3, YTH N6-methyladenosine RNA-binding protein F2, 3.

decrease in METTL3 protein levels, with no change in METTL3 mRNA levels, consistent with observations in AF patient samples (*Figure 7C* and *D*).

Since METTL3 was mainly degraded via the ubiquitin-proteasome pathway (see Supplementary material online, *Figure S1H*), we hypothesized that CREB1 loss might reduce the expression of a deubiquitinating enzyme, thus increasing the ubiquitination of METTL3. Analysis of transcription factor target genes across three databases (JASPAR,[33] ChEA,[34] and ENCODE[35]) revealed that CREB1 regulates several deubiquitinating enzymes, including USP15, USP2, USP20, USP5, and USP9X (*Figure 7E*). Among these, only USP9X showed significant down-regulation at both the mRNA and protein levels following CREB1 knockdown in HL-1 cells (*Figure 7F* and *G*). Furthermore, dual

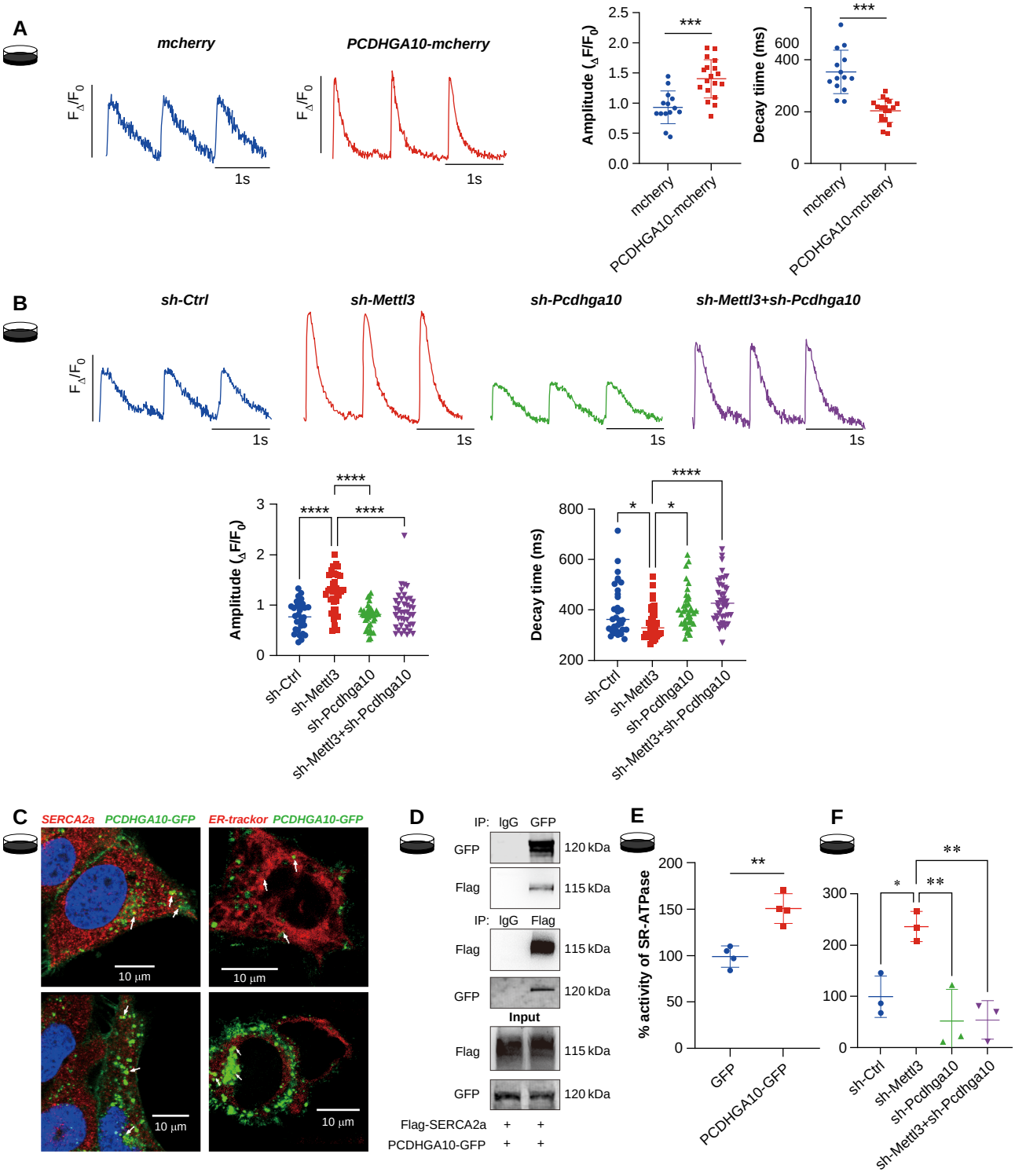

Figure 6 METTL3 affected calcium transients in atrial cardiomyocytes via PCDHGA10. (*A*) Calcium transients were detected by the confocal microscopy in PCDHGA10-mcherry and mcherry (control) NMAMs. Data are represented as mean ± SD. mcherry ($n = 14$ cells from three technical replicates), PCDHGA10-mcherry ($n = 18$ cells from three technical replicates). ***$P < 0.001$, comparisons made using unpaired Student's *t*-test. (*B*) Calcium transients were detected by the confocal microscopy in sh-Ctrl, sh-Mettl3, sh-Pcdhga10, and sh-Mettl3 + sh-Pcdhga10 NMAMs. Data are represented as mean ± SD. Sh-Ctrl ($n = 32$ cells from three technical replicates), sh-Mettl3 ($n = 39$ cells from three technical replicates), sh-Pcdhga10 ($n = 37$ cells from three technical replicates), and sh-Mettl3 + sh-Pcdhga10 ($n = 41$ cells from three technical replicates). *$P < 0.05$, ****$P < 0.0001$, comparisons made using two-way ANOVA. (*C*) Immunofluorescence staining with SERCA2a antibody was performed in NMAMs overexpressing PCDHGA10-GFP. The sarcoplasmic reticulum was demonstrated by the ER tracker-red. The white arrows show the sites where PCDHGA10

(continued)

luciferase reporter assays showed that CREB1 regulates USP9X transcription, as evidenced by increased USP9X promoter activity in the presence of Forskolin (a direct activator of cAMP) and a decrease in activity following treatment with KG-501 (a CREB1 inhibitor; see Supplementary material online, *Figure S10A* and *B*). Consistently, in AF patient samples, both USP9X mRNA and protein levels were significantly reduced (see Supplementary material online, *Figure S10C* and *D*). Knockdown of USP9X in HL-1 cells resulted in a significant decrease in METTL3 protein levels (*Figure 7H*) and an increased in METTL3 ubiquitination (*Figure 7I*). In summary, our findings suggested that the reduction of CREB1 and USP9X in AF contributes to increased ubiquitination and degradation of METTL3, thereby lowering its protein levels without affecting its mRNA expression.

Discussion

Main findings of this study

This present study, to the best of our knowledge, is the first to explore the relationship between METTL3 in atrial myocytes and AF. METTL3 protein was found to decrease during AF, and METTL3 deficiency was shown to promote AF development in experimental models. Mechanically, METTL3 deficiency led to enhanced calcium handling through increased PCDHGA10 expression in atrial myocytes.

METTL3 and cardiovascular diseases

As the predominant m^{6}A modification catalytic enzyme, METTL3 has been found to play critical roles in various cardiovascular diseases. For instance, METTL3 and m^{6}A modification are up-regulated in atherosclerosis, and METTL3 knockdown effectively prevents the atherogenic process by targeting NLRP3 and KLF4 mRNA.[36] METTL3 also plays a protective role in cardiac hypertrophy through regulation of PARP10 mRNA.[37] Additionally, METTL3 and m^{6}A modification are implicated in pulmonary hypertension,[38] aortic aneurysm, and dissection.[39] However, studies on m^{6}A modification and arrhythmias are limited. Carnevali *et al.*[40] reported that m^{6}A demethylase FTO knockout mice exhibited increased heart rhythm variability and susceptibility to premature ventricular contractions under stress. It has been reported that the up-regulation of METTL3 promotes cardiac fibroblast proliferation, thereby promoting cardiac fibrosis,[41] which is an important substrate for AF. Interestingly, our findings suggest that during AF, METTL3 is down-regulated in atrial myocytes. This contradictory regulation of METTL3 between atrial fibroblasts and myocytes may be due to the distinct metabolic remodelling observed in these cell types during AF. Atrial fibroblasts undergo mitochondrial biogenesis and enhanced cellular respiration,[42,43] while atrial myocytes experience impaired electron transport chain function, increased reactive oxygen species, and mitochondrial dysfunction.[44] METTL3's association with mitochondrial function warrants further investigation.[45,46]

Atrial cardiomyopathy and atrial fibrillation

Atrial cardiomyopathy (AtCM) refers to structural, architectural, contractile, or electrophysiological changes in the atria with potential clinical relevance. Atrial cardiomyopathy typically precedes AF, and early identification is key for prevention.[47] Our study revealed that increased KCNJ5 and disordered calcium handling in atrial myocytes, features of AtCM, are mechanisms by which METTL3 deficiency promotes AF.

$I_{K,ACh}$, an atrial-specific current, is primarily composed of KCNJ3 and KCNJ5 with a stoichiometric 2:2.[48] KCNJ5 alone can also form homotetramers,[49,50] which are activated by vagally released ACh. Structurally activated $I_{K,ACh}$ is implicated in chronic AF,[51,52] and $I_{K,ACh}$ blockers like tertiapin effectively inhibit the re-entry waves formation and terminate AF.[53]

By studying the calcium activity of atrial myocytes, we found that deficiency of METTL3 resulted in abnormal calcium handling through PCDHGA10 and SERCA2a in atrial myocytes. Increased expression of SERCA2a leads to sarcoplasmic reticulum calcium overload, heightening AF susceptibility.[54] While previous studies identified SERCA2a as a binding protein of PCDHGA10,[25] our study is the first to link PCDHGA10 to AF and its role in calcium handling.

In the past few decades, despite significant progress in AF research, mechanism-based treatments remain scarce.[5] Our findings highlight METTL3 deficiency as a pathogenic factor in AtCM and AF. Combined with advancements in m^{6}A modification interventions,[55] our research will bridge basic science and clinical translation, offering novel therapeutic targets for AF management.

CREB1/USP9X axis in heart disease

cAMP-responsive element-binding protein 1 (CREB1) is phosphorylated by cAMP-dependent protein kinase, enabling its nuclear entry and transcriptional activation.[56] CREB1 expression and transcriptional activity are reduced in AF patient LAAs,[30,31,57] consistent with our findings. We demonstrated that CREB1 regulates METTL3 protein levels indirectly via USP9X, a deubiquitinating enzyme. CREB1's role in regulating ubiquitination has been reported, with studies showing CREB1 increasing RCAN1 ubiquitination to promote degradation, a process mitigated by proteasome inhibitors.[58]

USP9X plays a protective role in heart diseases, as evidenced by its association with reduced congenital heart disease–related pulmonary arterial hypertension[59] and inhibition of aortic calcification.[60] Our findings suggest reduced USP9X expression in patients with AF aligns with its protective functions, proposing the CREB1/USP9X axis as a potential therapeutic target for AF.

Limitation

Our study still had some limitations. First, the precise mechanism by which PCDHGA10 affects SERCA2a activity remains unclear. Secondly, it is unknown whether METTL3 influences phosphorylation

Figure 6 Continued
colocalizes with SERCA2a and the sarcoplasmic reticulum. (*D*) Co-IP experiment of HEK293T cells overexpressing PCDHGA10-GFP and Flag-SERCA2a was performed with GFP and Flag antibodies, followed by western blotting experiments with GFP and Flag antibodies. (*E*) SERCA2a-ATPase activity measurement in HL-1 cells overexpressing PCDHGA10-GFP and GFP (Control). Data are represented as mean ± SD. GFP ($n = 4$), PCDHGA10-GFP ($n = 4$), comparison made using unpaired Student's *t*-test. (*F*) SERCA2a ATPase activity measurement in sh-Ctrl, sh-Mettl3, sh-Pcdhga10, and sh-Mettl3 + sh-Pcdhga10 HL-1 cells. Data are represented as mean ± SD. Sh-Ctrl ($n = 3$), sh-Mettl3 ($n = 3$), sh-Pcdhga10 ($n = 3$), and sh-Mettl3 + sh-Pcdhga10 ($n = 3$). *$P < 0.05$, **$P < 0.01$, comparisons made using two-way ANOVA. ANOVA, analysis of variance; GFP, green fluorescent protein; METTL3, methyltransferase like 3; NMAMs, neonatal mice atrial myocytes; PCDHGA10, protocadherin gamma subfamily A, 10; SERCA2a, SR Ca^{2+}-ATPase Type 2a; SD, standard deviation.

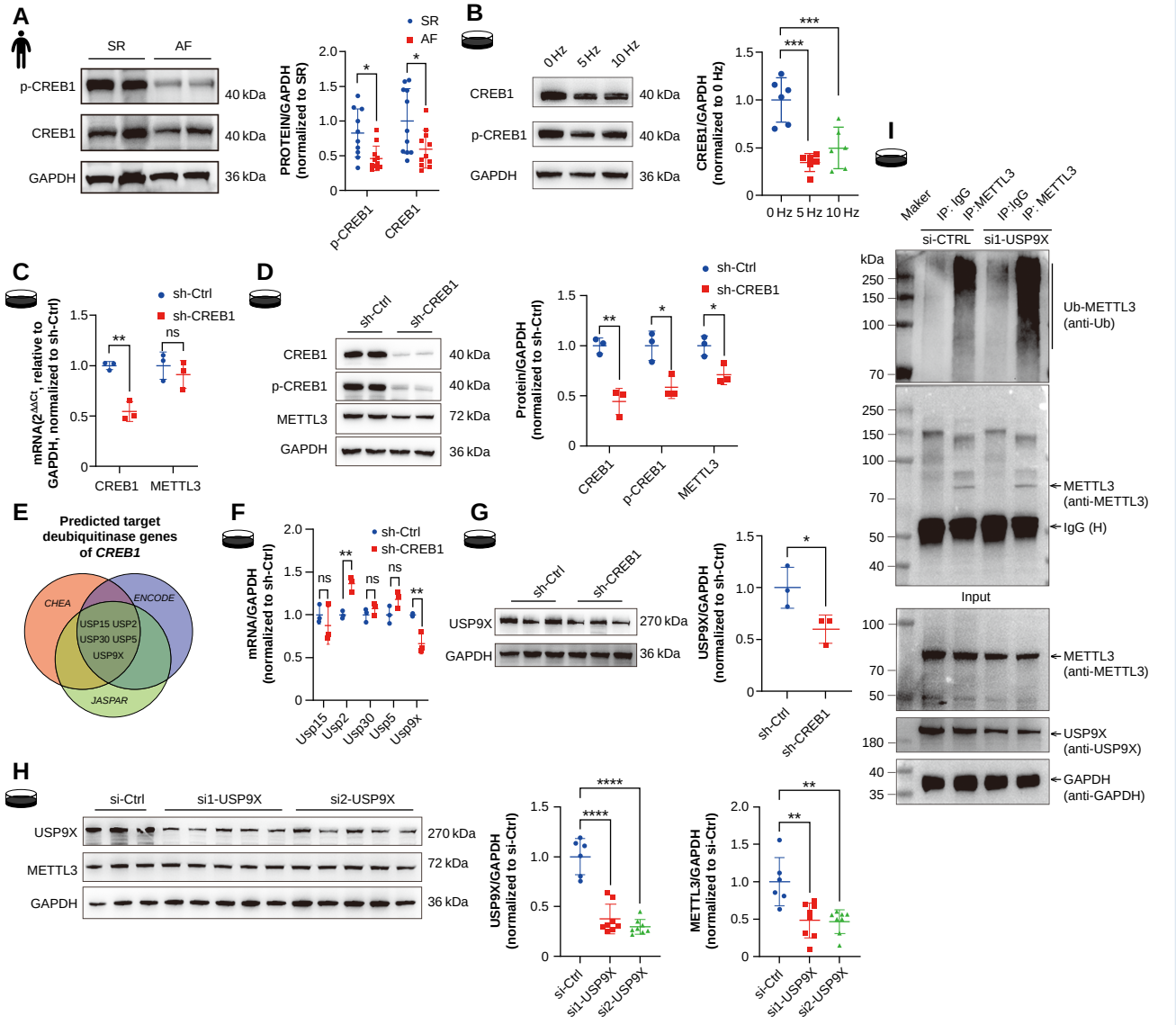

Figure 7 Reduced CREB1/USP9X axis in AF leads to decreased METTL3 protein. (*A*) Protein expression of p-CREB1 (S133) and CREB1 were detected by western blotting in LAA tissue of patients with AF. Data are represented as mean ± SD. SR ($n = 11$), AF ($n = 11$). $^{*}P < 0.05$, comparisons made using unpaired Student's *t*-test. (*B*) Protein expression of p-CREB1 (S133) and CREB1 in HL-1 cells at certain stimulation frequencies. Data are represented as mean ± SD. 0 Hz ($n = 6$), 5 Hz ($n = 6$), and 10 Hz ($n = 6$). $^{***}P < 0.001$, comparison made using ordinary one-way ANOVA. (*C*) CREB1 and METTL3 mRNA levels were detected by RT–qPCR in sh-Ctrl and sh-CREB1 HL-1 cells. Data are represented as mean ± SD. Sh-Ctrl ($n = 3$), sh-CREB1 ($n = 3$). $^{**}P < 0.01$, comparisons made using unpaired Student's *t*-test. (*D*) p-CREB1 (S133), CREB1, and METTL3 protein levels were detected by western blotting in sh-Ctrl and sh-CREB1 HL-1 cells. Data are represented as mean ± SD. Sh-Ctrl ($n = 3$), sh-CREB1 ($n = 3$). $^{*}P < 0.05$, $^{**}P < 0.01$, comparisons made using unpaired Student's *t*-test. (*E*) Prediction of CREB1 transcriptionally regulated deubiquitinases through ChEA, ENCODE, and JASPAR transcription factor databases. (*F*) USP15, USP2, USP30, USP5, and USP9X mRNA levels were evaluated by RT–qPCR in sh-Ctrl and sh-CREB1 HL-1 cells. Data are represented as mean ± SD. Sh-Ctrl ($n = 3$), sh-CREB1 ($n = 3$). $^{**}P < 0.01$, comparisons made using unpaired Student's *t*-test. (*G*) USP9X protein levels were detected by western blotting in sh-Ctrl and sh-CREB1 HL-1 cells. Data are represented as mean ± SD. Sh-Ctrl ($n = 3$), sh-CREB1 ($n = 3$). $^{*}P < 0.05$, comparisons made using unpaired Student's *t*-test. (*H*) USP9X, METTL3 protein levels were detected in si-Ctrl, si1-USP9X, and si2-USP9X HL-1 cells. Data are represented as mean ± SD. Si-Ctrl ($n = 6$), si1-USP9X ($n = 8$), si2-USP9X ($n = 8$). $^{**}P < 0.01$, $^{****}P < 0.0001$, comparisons made using ordinary one-way ANOVA. (*I*) The ubiquitination level of METTL3 in si-Ctrl and si1-USP9X HL-1 cells was detected. Endogenous IP was performed using METTL3 antibody or negative control rabbit IgG antibody, followed by western blotting. AF, atrial fibrillation; ANOVA, analysis of variance; CREB1, cAMP-responsive element-binding protein 1; GAPDH, glyceraldehyde-3-phosphate dehydrogenase; IgG, immunoglobulin G; IP, immunoprecipitation; LAA, left atrial appendage; METTL3, methyltransferase like 3; ns, not significant; RT–qPCR, reverse transcriptase–quantitative polymerase chain reaction; SD, standard deviation; SR, sinus rhythm.

or oxidative modifications of SERCA2a or other calcium ion channels. Thirdly, the potential effects of METTL3 on other ion channels besides KCNJ5 require further investigation.

Conclusions

In summary, our findings suggest that METTL3 plays a crucial role in AF development by influencing calcium handling in atrial myocytes. Additionally, the CREB1/USP9X axis is implicated in the down-regulation of METTL3 protein during AF. These findings provide insights into potential mechanism-based therapeutic targets for AF treatment.

Supplementary material

Supplementary material is available at *Europace* online.

Authors' contributions

D.-J.W. and Qin.Z. supervised and designed this study. Qia.Z. handled the revision comments, designed the experiment, and replied. J.S., X.-Y.Z., R.-H.Y., and W.-X.L. performed the cellular and molecular experiments. J.Y., L.T., and C.-Y.K. analysed the data. J.S. and X.-Y.Z. wrote the manuscript. H.-Q.L., F.C., and J.-J.W. helped with the human sample collection and animal studies. W.-S.X. and J.-L.F. performed additional experiments to reply to the comments.

Experimental ethics and consent

The use of human samples in this experiment was in compliance with the Declaration of Helsinki and was approved by the Institutional Review Board of Nanjing Drum Tower Hospital (2020-185-01). In addition, written consent was obtained from each included patient to remove and obtain the atrial appendages. All animal experiments were performed in accordance with the ARRIVE Guidelines and were approved by the Animal Care and Use Committee of Nanjing Drum Tower Hospital.

Funding

This work was supported by the Nanjing Medical Science and Technique Development Foundation (grant number ZKX21021), the National Natural Science Foundation of China (grant numbers 82241212, 82270346, and 82200356), and the China Postdoctoral Science Foundation (grant number 2024M761412).

Conflict of interest: none declared.

Data availability

Data underlying this article will be shared upon reasonable request with the corresponding author.

References

1. Brundel B, Ai X, Hills MT, Kuipers MF, Lip GYH, de Groot NMS. Atrial fibrillation. *Nat Rev Dis Primers* 2022;**8**:21.
2. Benz AP, Hohnloser SH, Eikelboom JW, Carnicelli AP, Giugliano RP, Granger CB *et al.* Outcomes of patients with atrial fibrillation and ischemic stroke while on oral anticoagulation. *Eur Heart J* 2023;**44**:1807–14.
3. Escudero-Martinez I, Morales-Caba L, Segura T. Atrial fibrillation and stroke: a review and new insights. *Trends Cardiovasc Med* 2023;**33**:23–9.
4. Schotten U, Verheule S, Kirchhof P, Goette A. Pathophysiological mechanisms of atrial fibrillation: a translational appraisal. *Physiol Rev* 2011;**91**:265–325.
5. Remme CA, Heijman J, Gomez AM, Zaza A, Odening KE. 25 Years of basic and translational science in EP Europace: novel insights into arrhythmia mechanisms and therapeutic strategies. *Europace* 2023;**25**:1–11.
6. Vinciguerra M, Dobrev D, Nattel S. Atrial fibrillation: pathophysiology, genetic and epigenetic mechanisms. *Lancet Reg Health Eur* 2024;**37**:100785.
7. Song D, Hou J, Wu J, Wang J. Role of N(6)-methyladenosine RNA modification in cardiovascular disease. *Front Cardiovasc Med* 2021;**8**:659628.
8. Fu Y, Dominissini D, Rechavi G, He C. Gene expression regulation mediated through reversible m(6)A RNA methylation. *Nat Rev Genet* 2014;**15**:293–306.
9. Tu B, Song K, Zhou Y, Sun H, Liu ZY, Lin LC *et al.* METTL3 boosts mitochondrial fission and induces cardiac fibrosis by enhancing LncRNA GAS5 methylation. *Pharmacol Res* 2023;**194**:106840.
10. Adili A, Zhu X, Cao H, Tang X, Wang Y, Wang J *et al.* Atrial fibrillation underlies cardiomyocyte senescence and contributes to deleterious atrial remodeling during disease progression. *Aging Dis* 2022;**13**:298–312.
11. Zhang D, Hu X, Li J, Liu J, Baks-Te Bulte L, Wiersma M *et al.* DNA damage-induced PARP1 activation confers cardiomyocyte dysfunction through NAD(+) depletion in experimental atrial fibrillation. *Nat Commun* 2019;**10**:1307.
12. Zhao ZY, Guo YM. Cacl2–ACh induced atrial fibrillation (flutter) in mice. *Zhongguo Yao Li Xue Bao* 1982;**3**:185–8.
13. Wei F, Ren W, Zhang X, Wu P, Fan J. miR-425-5p is negatively associated with atrial fibrosis and promotes atrial remodeling by targeting CREB1 in atrial fibrillation. *J Cardiol* 2022;**79**:202–10.
14. Fu Y, Jiang T, Sun H, Li T, Gao F, Fan B *et al.* Necroptosis is required for atrial fibrillation and involved in aerobic exercise-conferred cardioprotection. *J Cell Mol Med* 2021;**25**:8363–75.
15. Muller FU, Lewin G, Baba HA, Boknik P, Fabritz L, Kirchhefer U *et al.* Heart-directed expression of a human cardiac isoform of cAMP-response element modulator in transgenic mice. *J Biol Chem* 2005;**280**:6906–14.
16. Ni L, Lahiri SK, Nie J, Pan X, Abu-Taha I, Reynolds JO *et al.* Genetic inhibition of nuclear factor of activated T-cell c2 prevents atrial fibrillation in CREM transgenic mice. *Cardiovasc Res* 2022;**118**:2805–18.
17. Yao C, Veleva T, Scott L Jr, Cao S, Li L, Chen G *et al.* Enhanced cardiomyocyte NLRP3 inflammasome signaling promotes atrial fibrillation. *Circulation* 2018;**138**:2227–42.
18. Ni L, Scott L Jr, Campbell HM, Pan X, Alsina KM, Reynolds J *et al.* Atrial-specific gene delivery using an adeno-associated viral vector. *Circ Res* 2019;**124**:256–62.
19. Verkerk AO, Geuzebroek GS, Veldkamp MW, Wilders R. Effects of acetylcholine and noradrenalin on action potentials of isolated rabbit sinoatrial and atrial myocytes. *Front Physiol* 2012;**3**:174.
20. Butova X, Myachina T, Simonova R, Kochurova A, Bozhko Y, Arkhipov M *et al.* Peculiarities of the acetylcholine action on the contractile function of cardiomyocytes from the left and right atria in rats. *Cells* 2022;**11**:1–15.
21. Boulias K, Greer EL. Biological roles of adenine methylation in RNA. *Nat Rev Genet* 2023;**24**:143–60.
22. Zou Z, He C. The YTHDF proteins display distinct cellular functions on m(6)A-modified RNA. *Trends Biochem Sci* 2024;**49**:611–21.
23. Chen WV, Alvarez FJ, Lefebvre JL, Friedman B, Nwakeze C, Geiman E *et al.* Functional significance of isoform diversification in the protocadherin gamma gene cluster. *Neuron* 2012;**75**:402–9.
24. Kiefer L, Chiosso A, Langen J, Buckley A, Gaudin S, Rajkumar SM *et al.* WAPL functions as a rheostat of protocadherin isoform diversity that controls neural wiring. *Science* 2023;**380**:eadf8440.
25. Han MH, Lin C, Meng S, Wang X. Proteomics analysis reveals overlapping functions of clustered protocadherins. *Mol Cell Proteomics* 2010;**9**:71–83.
26. Hamilton S, Terentyev D. Proarrhythmic remodeling of calcium homeostasis in cardiac disease; implications for diabetes and obesity. *Front Physiol* 2018;**9**:1517.
27. Shah S, Akhtar MS, Hassan MQ, Akhtar M, Paudel YN, Najmi AK. EGFR tyrosine kinase inhibition decreases cardiac remodeling and SERCA2a/NCX1 depletion in streptozotocin induced cardiomyopathy in C57/BL6 mice. *Life Sci* 2018;**210**:29–39.
28. Callewaert G, Cleemann L, Morad M. Caffeine-induced Ca^{2+} release activates Ca^{2+} extrusion via Na^{+}-Ca^{2+} exchanger in cardiac myocytes. *Am J Physiol* 1989;**257**:C147–52.
29. Sitsapesan R, Williams AJ. Mechanisms of caffeine activation of single calcium-release channels of sheep cardiac sarcoplasmic reticulum. *J Physiol* 1990;**423**:425–39.
30. Deshmukh A, Barnard J, Sun H, Newton D, Castel L, Pettersson G *et al.* Left atrial transcriptional changes associated with atrial fibrillation susceptibility and persistence. *Circ Arrhythm Electrophysiol* 2015;**8**:32–41.
31. Moreira LM, Takawale A, Hulsurkar M, Menassa DA, Antanaviciute A, Lahiri SK *et al.* Paracrine signalling by cardiac calcitonin controls atrial fibrogenesis and arrhythmia. *Nature* 2020;**587**:460–5.
32. Chen J, Qin H, Hao J, Wang Q, Chen S, Yang G *et al.* Cardiac-specific overexpression of CREM-IbDeltaC-X via CRISPR/Cas9 in mice presents a new model of atrial cardiomyopathy with spontaneous atrial fibrillation. *Transl Res* 2024;**267**:54–66.
33. Castro-Mondragon JA, Riudavets-Puig R, Rauluseviciute I, Lemma RB, Turchi L, Blanc-Mathieu R *et al.* JASPAR 2022: the 9th release of the open-access database of transcription factor binding profiles. *Nucleic Acids Res* 2022;**50**:D165–73.
34. Lachmann A, Xu H, Krishnan J, Berger SI, Mazloom AR, Ma'ayan A. ChEA: transcription factor regulation inferred from integrating genome-wide ChIP-X experiments. *Bioinformatics* 2010;**26**:2438–44.

35. Hu H, Miao YR, Jia LH, Yu QY, Zhang Q, Guo AY. AnimalTFDB 3.0: a comprehensive resource for annotation and prediction of animal transcription factors. *Nucleic Acids Res* 2019;**47**:D33–8.
36. Chien CS, Li JY, Chien Y, Wang ML, Yarmishyn AA, Tsai PH *et al.* METTL3-dependent N(6)-methyladenosine RNA modification mediates the atherogenic inflammatory cascades in vascular endothelium. *Proc Natl Acad Sci U S A* 2021;**118**:1–12.
37. Gao XQ, Zhang YH, Liu F, Ponnusamy M, Zhao XM, Zhou LY *et al.* The piRNA CHAPIR regulates cardiac hypertrophy by controlling METTL3-dependent N(6)-methyladenosine methylation of Parp10 mRNA. *Nat Cell Biol* 2020;**22**:1319–31.
38. Xu S, Xu X, Zhang Z, Yan L, Zhang L, Du L. The role of RNA m(6)A methylation in the regulation of postnatal hypoxia-induced pulmonary hypertension. *Respir Res* 2021;**22**:121.
39. Li T, Wang T, Jing J, Sun L. Expression pattern and clinical value of key m6A RNA modification regulators in abdominal aortic aneurysm. *J Inflamm Res* 2021;**14**:4245–58.
40. Carnevali L, Graiani G, Rossi S, Al Banchaabouchi M, Macchi E, Quaini F *et al.* Signs of cardiac autonomic imbalance and proarrhythmic remodeling in FTO deficient mice. *PLoS One* 2014;**9**:e95499.
41. Zhou Y, Song K, Tu B, Sun H, Ding JF, Luo Y *et al.* METTL3 boosts glycolysis and cardiac fibroblast proliferation by increasing AR methylation. *Int J Biol Macromol* 2022;**223**: 899–915.
42. Bernard K, Logsdon NJ, Ravi S, Xie N, Persons BP, Rangarajan S *et al.* Metabolic reprogramming is required for myofibroblast contractility and differentiation. *J Biol Chem* 2015;**290**:25427–38.
43. Negmadjanov U, Godic Z, Rizvi F, Emelyanova L, Ross G, Richards J *et al.* TGF-beta1-mediated differentiation of fibroblasts is associated with increased mitochondrial content and cellular respiration. *PLoS One* 2015;**10**:e0123046.
44. Bode D, Pronto JRD, Schiattarella GG, Voigt N. Metabolic remodelling in atrial fibrillation: manifestations, mechanisms and clinical implications. *Nat Rev Cardiol* 2024;**21**: 682–700.
45. Yang L, Pang X, Guo W, Zhu C, Yu L, Song X *et al.* An exploration of the coherent effects between METTL3 and NDUFA10 on Alzheimer's disease. *Int J Mol Sci* 2023;**24**: 1–16.
46. He J, Hao F, Song S, Zhang J, Zhou H, Zhang J *et al.* METTL family in healthy and disease. *Mol Biomed* 2024;**5**:33.
47. Goette A, Corradi D, Dobrev D, Aguinaga L, Cabrera JA, Chugh SS *et al.* Atrial cardiomyopathy revisited-evolution of a concept: a clinical consensus statement of the European Heart Rhythm Association (EHRA) of the ESC, the Heart Rhythm Society (HRS), the Asian Pacific Heart Rhythm Society (APHRS), and the Latin American Heart Rhythm Society (LAHRS). *Europace* 2024;**26**:1–31.
48. Cui M, Cantwell L, Zorn A, Logothetis DE. Kir channel molecular physiology, pharmacology, and therapeutic implications. *Handb Exp Pharmacol* 2021;**267**:277–356.
49. Wickman K, Nemec J, Gendler SJ, Clapham DE. Abnormal heart rate regulation in GIRK4 knockout mice. *Neuron* 1998;**20**:103–14.
50. Cui M, Xu K, Gada KD, Shalomov B, Ban M, Eptaminitaki GC *et al.* A novel small-molecule selective activator of homomeric GIRK4 channels. *J Biol Chem* 2022;**298**: 102009.
51. Dobrev D, Friedrich A, Voigt N, Jost N, Wettwer E, Christ T *et al.* The G protein-gated potassium current I(K,ACh) is constitutively active in patients with chronic atrial fibrillation. *Circulation* 2005;**112**:3697–706.
52. Voigt N, Friedrich A, Bock M, Wettwer E, Christ T, Knaut M *et al.* Differential phosphorylation-dependent regulation of constitutively active and muscarinic receptor-activated IK,ACh channels in patients with chronic atrial fibrillation. *Cardiovasc Res* 2007; **74**:426–37.
53. Bingen BO, Neshati Z, Askar SF, Kazbanov IV, Ypey DL, Panfilov AV *et al.* Atrium-specific Kir3.x determines inducibility, dynamics, and termination of fibrillation by regulating restitution-driven alternans. *Circulation* 2013;**128**:2732–44.
54. Herraiz-Martinez A, Llach A, Tarifa C, Gandia J, Jimenez-Sabado V, Lozano-Velasco E *et al.* The 4q25 variant rs13143308T links risk of atrial fibrillation to defective calcium homoeostasis. *Cardiovasc Res* 2019;**115**:578–89.
55. Selberg S, Blokhina D, Aatonen M, Koivisto P, Siltanen A, Mervaala E *et al.* Discovery of small molecules that activate RNA methylation through cooperative binding to the METTL3-14-WTAP complex active site. *Cell Rep* 2019;**26**:3762–71.
56. Mayr B, Montminy M. Transcriptional regulation by the phosphorylation-dependent factor CREB. *Nat Rev Mol Cell Biol* 2001;**2**:599–609.
57. Wang Y, Cai W, Gu L, Ji X, Shen Q. Comprehensive analysis of pertinent genes and pathways in atrial fibrillation. *Comput Math Methods Med* 2021;**2021**:4530180.
58. Seo SR, Chung KC. CREB activates proteasomal degradation of DSCR1/RCAN1. *FEBS Lett* 2008;**582**:1889–93.
59. Reijnders MR, Zachariadis V, Latour B, Jolly L, Mancini GM, Pfundt R *et al.* De novo loss-of-function mutations in USP9X cause a female-specific recognizable syndrome with developmental delay and congenital malformations. *Am J Hum Genet* 2016;**98**:373–81.
60. Majumdar U, Manivannan S, Basu M, Ueyama Y, Blaser MC, Cameron E *et al.* Nitric oxide prevents aortic valve calcification by S-nitrosylation of USP9X to activate NOTCH signaling. *Sci Adv* 2021;**7**:1–15.